analytical chemistry

Article

Cite This: *Anal. Chem.* 2019, 91, 12315−12320

pubs.acs.org/ac

Laser Spectroscopy for Monitoring of Radiocarbon in Atmospheric Samples

Guillaume Genoud,*[,†] Johannes Lehmuskoski,[†] Steven Bell,[‡] Vesa Palonen,[§] Markku Oinonen,[∥] Mari-Leena Koskinen-Soivi,[†] and Matti Reinikainen[†]

[†]VTT Technical Research Centre of Finland Limited, Espoo FI-02044 VTT, Finland

[‡]National Physical Laboratory, Hampton Road, Teddington, Middlesex TW11 0LW, United Kingdom

[§]Department of Physics and [∥]Finnish Museum of Natural History, University of Helsinki, P.O. Box 64, 00014 Helsinki, Finland

ABSTRACT: In-situ monitoring of radiocarbon emissions is challenging due to the lack of a suitable method for sensitive online detection of this isotope. Here we report on a complete system for automatized continuous on-site monitoring of radiocarbon gaseous emissions from nuclear facilities. By combining radiocarbon detection using mid-infrared cavity ring-down spectroscopy and an advanced sampling system, an elevated amount of radiocarbon in an atmospheric-like gas matrix was detected. Radiocarbon was detected in the form of $^{14}CO_2$ after extraction of the carbon dioxide from the air sample. The system is also able to discriminate between radiocarbon in organic or inorganic molecular form by converting $^{14}CH_4$ into $^{14}CO_2$. This work lays the groundwork for further use of this technology in nuclear facilities for online on-site monitoring of radioactive gaseous emissions as well as future work on in-situ monitoring of atmospheric radiocarbon.

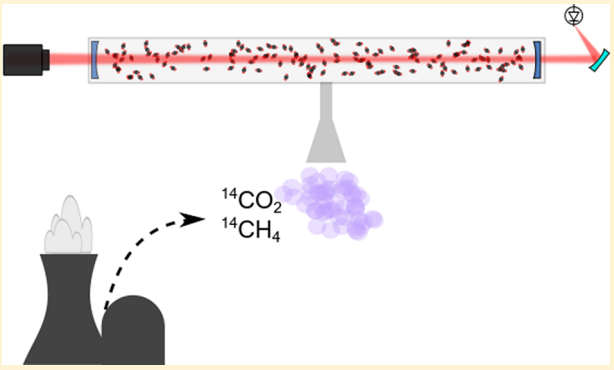

Long-lived radionuclides, such as radiocarbon (C-14), are problematic because they have a high residence time in the environment and can easily be assimilated into living matter.[1] They are the main source of radioactive gas emissions in nuclear facilities, are highly mobile in the environment, and, due to their long half-life (5700 years for C-14[2,3]), require long-term monitoring. These radionuclides are particularly challenging to detect on-site, as current methods are based on laboratory-based detection techniques. Rapid continuous in-situ analysis would be valuable as it can provide better monitoring capabilities in support of power plant operators, nuclear waste management organizations, and regulators.

Radiocarbon is present in all parts of nuclear power plants, where it is one of the main sources of radioactive gaseous emissions, mostly in the form of carbon dioxide or methane, for instance, produced through the biodegration of radioactive waste.[4] Operational gaseous emissions take place inside nuclear facilities, and radiocarbon is emitted through the stack air with a C-14 activity concentration in the range 200−400 Bq/m^3.[5] Gaseous radiocarbon monitoring currently requires a long collection time and lengthy radiochemistry analysis before determining its concentration, for instance, using liquid scintillation counting (LSC). In recent years, optical detection of radiocarbon in the form of $^{14}CO_2$ has been successfully demonstrated, and low detection limits were achieved.[6−11] These measurements were performed with samples containing pure CO_2, which is rarely the case in nuclear facilities. In this article, we report on work toward in-situ continuous monitoring of C-14 emissions in the form of carbon dioxide and methane. Those molecules are detected using an optical method after extraction of the carbon dioxide from an air-like matrix.

Optical detection of C-14 offers several advantages over conventionally used techniques for nuclear applications, such as LSC, which is commonly used for laboratory analysis in nuclear facilities. LSC requires sample collection and off-line analysis and in most cases is not suitable for on-site monitoring. Gaseous samples must be trapped in liquid form and bound to the medium, which will produce additional radioactive waste. Additionally, scintillation peaks of different radionuclides typically overlap in LSC spectra, thus limiting its sensitivity and often requiring time-consuming radiochemistry methods to separate the different beta emitters.

Laser spectroscopy can circumvent most of these issues. It analyzes directly gaseous samples, thus producing no additional waste. The use of an optical technique also enables compact, automated, and cost-effective instruments to be built, ideal for online in-situ monitoring. The method is selective and will only be sensitive to one radionuclide, meaning that the radiocarbon content can easily be determined even if the sample contains other radionuclides. The method also detects only one molecular form and thus provides a means to

Received: May 30, 2019
Accepted: September 10, 2019
Published: September 10, 2019

DOI: 10.1021/acs.analchem.9b02496
Anal. Chem. 2019, 91, 12315−12320

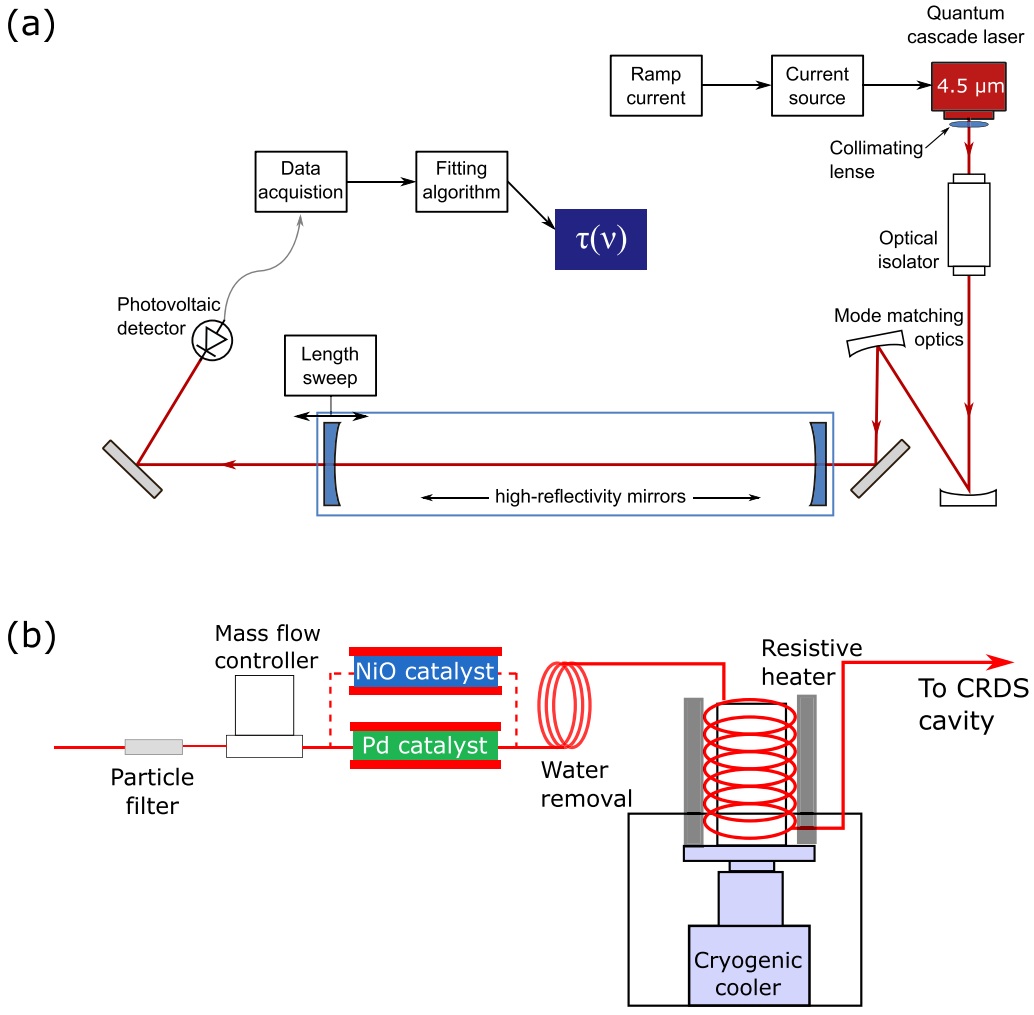

Figure 1. Schematic of the experimental arrangement. The instrumentation consist of two parts. (a) CRDS system to detect $^{14}CO_2$. A current ramp is applied to the QCL to scan its wavelength, ν, and the corresponding ring-down time as a function of wavelength, $\tau(\nu)$, is determined, allowing one to deduce the concentration of each gas species. (b) Sampling system to extract CO_2 from air and convert organic C-14 into CO_2.

determine its speciation. In the case of radiocarbon, $^{14}CO_2$ is detected while other organic species such as $^{14}CH_4$ are not. Organic C-14 is more easily assimilated by living organisms and its monitoring is pertinent. While most work on optical detection of C-14 has so far focused on $^{14}CO_2$ detection, direct optical detection of other molecules, such as $^{14}CH_4$, can also be envisioned.[12] Other radionuclides such as tritium, in the form of tritiated water, can also be detected using laser spectroscopy[13] and can, in the future, be combined with radiocarbon detection.

Radiocarbon detection also has numerous applications in other fields of science. It is present in a trace amount in the atmosphere with a natural abundance of $^{14}C/C = 1.2$ ppt, and all carbon of biogenic origin has the same isotopic abundance. On the other hand, carbon of fossil origin does not contain any radiocarbon, being millions of years old and having completely decayed. C-14 is thus the ideal tracer to discriminate between emissions of fossil or biogenic origin and can be used for biofraction determination,[14,15] carbon dating, or apportion of emissions sources. It is commonly used in biomedicine to label compounds for drug development. In those cases, accelerator mass spectrometry (AMS) is used as it can deliver extremely high sensitivity, but it usually requires complex sample preparation and is not suitable for in-situ measurements. Optical methods can therefore also provide an alternative to AMS for C-14 detection.[11,16] The results presented here contribute to demonstrate the viability of the method for on-site measurements of low levels of C-14 in the atmosphere as issues associated with the analysis of radiocarbon in atmospheric samples are addressed.

METHODS

Overview. In typical samples from nuclear facilities the CO_2 concentration ranges from 400 ppm to a few percent, while the $^{14}C/C$ ratio is in the range 1−100 ppb. This corresponds to activity values in the range from 40 Bq/m^3 to 100 kBq/m^3. The amount of methane significantly varies but can reach values similar to $^{14}CO_2$. In most cases, detection of $^{14}CO_2$ with the optical method is thus not feasible without first concentrating the CO_2. The C-14 monitoring system consists therefore of two parts: a sampling module to extract CO_2 from air and convert methane into carbon dioxide and a laser spectroscopy module to detect trace amounts of $^{14}CO_2$, which is based on the cavity ring-down spectroscopy (CRDS) technique, as illustrated in Figure 1a. In CRDS, the ring-down time, τ, is recorded at each wavelength and by comparing it with the vacuum ring-down time, τ_0, the sample absorption spectrum is computed. If the line strength is known,

DOI: 10.1021/acs.analchem.9b02496
Anal. Chem. 2019, 91, 12315−12320

the gas concentration can be inferred. A quantum cascade laser (QCL) is used as a light source and coupled to a 40 cm long cavity composed of high-reflectivity mirrors (>99.97%). The cavity used in this work has a vacuum ring-down time of 5.2 μs. Light is detected by a photovoltaic detector at the output of the cavity. By using these components one can achieve high sensitivity in a compact setup with a footprint of 45 cm × 60 cm. The strongest absorption band for the detection of $^{14}CO_2$ corresponds to the fundamental asymmetric stretching vibration band ν_3. The P20e transition situated at 2209.11 cm^{-1} (or 4.52 μm) is used in this work, as it has been shown to be the most suitable line, with minimum interferences from other isotopes.[17−20] The CRDS system was described in more detail in our previous publication, where it was characterized using pure CO_2.[7]

Sampling Unit. The sampling unit is composed of two main parts: a cryogenic trap to extract the CO_2 out of air and a catalytic conversion reactor to convert organic carbon into carbon dioxide in order to differentiate between these two types of radioactive emissions. CO_2 extraction from air samples is achieved by freezing the CO_2 in a trap cooled down to below the freezing point of CO_2 (195 K). By subsequently heating the trap to a temperature above this, almost pure CO_2 is produced which can then be analyzed using laser spectroscopy. The trapping system is based on designs by Miller et al.[21] and Mohn et al.[22] The trap consists of 1/16″ stainless steel tubing coiled around a copper piece, which is cooled down by a cryogenic cooler, as shown in Figure 1b. The cryogenic cooler is a Brooks PCC Compact Cooler, which does not require any liquid nitrogen, and is thus ideal for future on-site measurements. To prevent clogging the trap with water ice, it is essential to remove water vapor before flowing the sample through the trap. This is achieved using a Nafion dryer and magnesium perchlorate. An extraction sequence typically consist of 15−30 min at low temperature (around 150 K), where the sample flows at 0.1−0.2 L/min through the trap. The trap inlet is then closed, and the remaining air in the trap is removed by pumping it to vacuum for a few minutes. The trap is then resistively heated until it reaches 230 K to release the frozen CO_2 into the CRDS cell, which has been pumped to vacuum beforehand. The pressure reached in the CRDS cell is measured with a capacitance manometer. Note that after a few cycles water accumulates in the trap, and it is then necessary to heat it to room temperature in order to remove the water ice clogging the tubing. The trap is able to extract a maximum of 10−15 mg of CO_2 in each cycle. In this way, almost pure CO_2 (>90%) is directed into the measurement cell, allowing for $^{14}CO_2$ detection using laser spectroscopy. During the CRDS measurement, trapping of a new sample is initiated with the trap cooling down again and the collection of the next sample starting. The whole sampling cycle is automatized using solenoid valves controlled by LabView.

Organic carbon, such as $^{14}CH_4$, is detected by converting CH_4 into CO_2 using catalytic conversion.[23] By performing two measurements, with and without catalytic conversion, it is possible to determine the amount of C-14 in the form of CO_2 or CH_4. For this purpose a palladium catalyst was used, which achieves efficient oxidation above 300 °C. In our system, the reactor was operated above 500 °C and a conversion efficiency close to 100% was achieved. The Pd catalyst was prepared on alumina carrier with 2.2 wt % of Pd according to the method described by Fouladvand et al.[24] The sample flows through 0.5 mL of catalyst before being directed through the water removal section and finally into the cryogenic trap where CO_2 freezes.

N_2O Removal. In most atmospheric-like samples, N_2O is also present in a trace amount (330 ppb). Unfortunately N_2O has a freezing point (182 K) very close to the freezing point of CO_2. With the current design, the cold source is attached to the bottom of the trap, resulting in a temperature gradient along the axis of the trap. It is thus difficult to control the trap temperature and achieve a homogeneous trap temperature, resulting in N_2O also being trapped. N_2O has strong absorption lines in the wavelength region at which $^{14}CO_2$ is detected, which will then interfere with the measurement. It is thus necessary to remove N_2O in order to achieve the highest sensitivity. In this work, this is achieved by oxidizing N_2O into N_2O_x with $x \geq 2$ using catalytic conversion. This reaction also occurs with the Pd catalyst, but it is necessary to have an another catalyst, which can selectively convert N_2O without converting methane into CO_2, in order to maintain the capability of differentiating the molecular forms of radiocarbon. It was found that a NiO catalyst was selectively converting N_2O and could be used for this application. The particular form of the NiO catalyst was a NiO/NaOH catalyst prepared according to the method described by Yu et al.,[25] and 0.5 mL of this catalyst was used.

Many parameters affects the amounts of trapped CO_2 and residual N_2O. Increased trapping time or flow rate will increase the amount of trapped CO_2. N_2O removal is linearly dependent with the volume of catalyst and inversely dependent on the flow rate. A smaller flow rate will thus result in a more efficient N_2O removal. The chosen flow rate is therefore a compromise between amount of CO_2 trapped and N_2O removal. The catalyst temperature also influences N_2O removal, and higher temperatures will more efficiently remove N_2O.

This is illustrated in Figure 2a, where the absorption spectra recorded with the CRDS system with different trapping parameters are presented. The samples were collected using laboratory air flowing through the cryogenic trap for 30 min and analyzed with the CRDS system. The spectra were recorded in the wavelength range 2208.95−2209.05 cm^{-1}, where absorption lines of both CO_2 and N_2O are present. The different absorption lines were identified using the HITRAN database.[26] The different sampling parameters and resulting CO_2 and N_2O concentration are summarized in Table 1. While the CO_2 concentration remains constant around 90%, the amount of trapped CO_2 increases as the flow rates increase, and higher pressure in the measurement cell is reached. The remaining 5−10% mostly consists of air (with an elevated amount of N_2O and water) which remains in the trap after flowing the air sample and, in some cases, is not properly flushed out. A larger flow rate will result in more N_2O being trapped because the catalytic conversion of N_2O is less efficient at larger flow rates. Finally, the conversion efficiency also depends on the temperature of the catalyst, and a lower concentration of N_2O is present at higher catalyst temperatures.

The optical measurement itself is fast (typically a few minutes), but the overall analysis time is limited by the trapping time which is relatively long. With the current configuration, a full measurement sequence ($^{14}CO_2$ and $^{14}CH_4$ analysis) takes 1.5 h. While this is a long time, it is still an order of magnitude shorter than currently used techniques, where sample collection and analysis can take several days. In this first

DOI: 10.1021/acs.analchem.9b02496
Anal. Chem. 2019, 91, 12315−12320

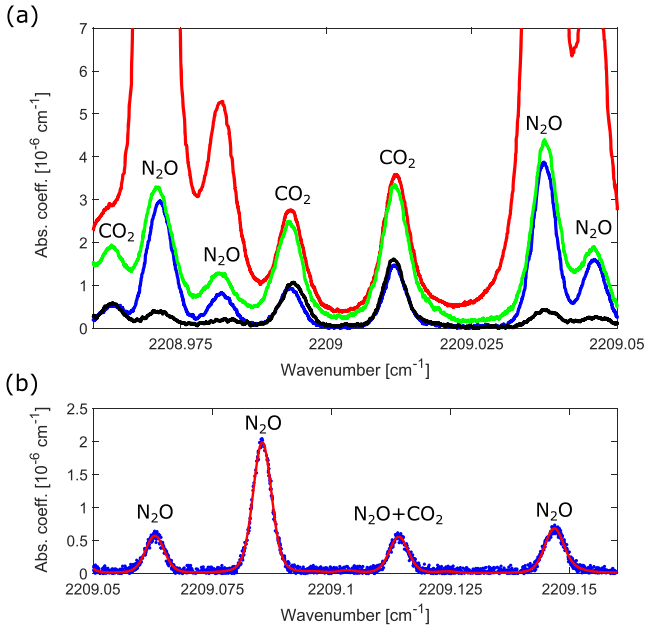

Figure 2. Air sample analyzed with the system. (a) Spectra recorded with different parameters of the sampling system listed in Table 1 (red, flow rate of 0.35 L/min and catalyst temperature of 450 °C; green, 0.35 L/min and 550 °C; blue, 0.1 L/min and 450 °C; black, 0.1 L/min and 550 °C). (b) Spectrum of trapped CO_2 from an air sample with a sample flow of 0.2 L/min and catalyst temperature of 600 °C. Red line is the corresponding fit using a sum of Voigt profiles. In a and b, each transition is labeled with the corresponding gas species. N_2O+CO_2 refers to a peak consisting of two overlapping lines of CO_2 and N_2O.

Table 1. CO_2 and N_2O Concentration as a Function of Different Sampling Parameters

curve	red	green	blue	black
pressure [mbar]	11.8	11.3	4	4.4
flow rate [L/min]	0.35	0.35	0.1	0.1
catalyst temperature [°C]	450	550	450	550
CO_2 concentration	0.93	0.97	0.89	0.90
N_2O concentration [ppm]	303	72	115	26

prototype, the sampling cycle duration is limited for mainly two reasons. First, the volume and weight of the trap is relatively large, requiring long times for cooling down and heating. The cavity volume is 180 mL, which is larger than necessary, and longer trapping times are needed in order to freeze sufficient CO_2. Second, to achieve optimum N_2O removal, low flow rates are used, which increases the trapping time. A shorter sampling time can be achieved by reducing the sampling cell volume and the weight of the trap and by increasing the amount of catalyst, which will allow one to increase the flow rate while keeping similar N_2O removal capabilities.

Figure 2b shows a measurement carried out using laboratory air with optimum trapping parameters around the 2209.1 cm^{-1} region where the P20e line of $^{14}CO_2$ is situated. The sample was circulating at 0.2 L/min through the cryogenic trap for 15 min, and a CO_2 pressure of 5.1 mbar was reached in the CRDS cell. As expected, no $^{14}CO_2$ is observed, as the atmostpheric C-14 concentration of 1.2 ppt is below the sensitivity limit of our instrumentation. With increased sensitivity and improved N_2O removal, atmospheric radiocarbon content monitoring can be achieved in the future with a similar system, which is of great importance for climate sciences.[27,28]

The positions of the residual N_2O absorption lines are used to give an absolute calibration for the wavenumber scale of the QCL. In particular, the lines situated at 2209.063, 2209.085, and 2209.147 cm^{-1}, observed in Figure 2b, are used to calibrate the wavelength scale of spectra recorded around the targeted $^{14}CO_2$ line.

RESULTS

To further test the system, a standardized sample was prepared by the National Physical Laboratory with an elevated amount of $^{14}CO_2$ and $^{14}CH_4$ in an air matrix, similar to what could be expected from outgasing of nuclear waste or nuclear power plant stack emissions. The samples were prepared from concentrated $^{14}CO_2$ and $^{14}CH_4$, which were subsequently pressurized with stable CO_2 and CH_4, respectively. The standardized activity concentrations of these master cylinders were 15.56 ± 0.32 and 175.7 ± 3.0 MBq/m^3, determined by absolute internal-gas proportional counting. The samples were mixed, further diluted gravimetrically, and pressurized with a known mass of compressed dry air. The final C-14 concentration of the sample was thus 339 ± 30 Bq/m^3 for $^{14}CO_2$ and 208 ± 18 Bq/m^3 for $^{14}CH_4$. The gas composition and purity of the samples were not directly measured.

To fully determine the absolute amount of $^{14}CO_2$ and $^{14}CH_4$ of the sample, 6 different measurements are necessary. First, measurements without CO_2 extraction through the cryogenic trap are carried out to determine the total amount of carbon dioxide and methane in the sample. These measurements are carried out with and without catalytic conversion. Two absorption lines of $^{13}C^{16}O_2$ situated at 2209.93 and 2209.95 cm^{-1} are used, and the concentration of CO_2 in the sample or CO_2+CH_4, c_3, is obtained. These measurements are fast (<1 min) as CO_2 trapping is not required.

Another set of measurements is then carried out with the sample flowing through the cryogenic trap where CO_2 is extracted. Those measurements are also performed with and without catalytic conversion. The laser is tuned to the wavelength region where the $^{14}CO_2$ line is situated at 2209.1 cm^{-1} to determine the concentration of C-14, c_1. Finally, by tuning the laser to absorption lines of stable CO_2 isotopes ($^{12}C^{16}O_2$), the concentration of CO_2 in the trap, c_2, is obtained using the CO_2 line situated at 2209.0116 cm^{-1} in Figure 2a. Using the line areas obtained from the fits and the known absorption line strength of the transitions, the gas concentrations are determined by $c_i = A_i k_B T/(S_{0i}(T)p)$, where A_i is the line area of the targeted absorption line, S_{0i} its line strength, k_B the Boltzmann constant, T the temperature of the sample, and p the sample pressure. The transition intensitiy of the P20e line of $^{14}CO_2$, $S_{01} = 2.8 \times 10^{-18}$ $cm^{-1}/(molecules\ cm^{-2})$, was previously determined by Zak et al. using ab initio quantum chemistry methods.[20] The same method was used by Zak et al. to calculate the values for S_{02}[29] and S_{03}[20] which are used here. The absolute amount of C-14 in the sample is then $c = c_1c_3/c_2$.

The system was used to analyze the standardized samples, and the obtained spectra are shown in Figure 3. In Figure 3a, the sample was flowing through the NiO catalyst, while in Figure 3c it was flowing trough the Pd catalyst, thus converting organic carbon into CO_2. In both cases, the trapping time was 30 min, the flow rate 0.2 L/min, and the catalyst temperature 600 °C. The spectra were recorded for 5 min with a data acquisition rate of about 35 Hz, resulting in about 10 000

DOI: 10.1021/acs.analchem.9b02496
Anal. Chem. 2019, 91, 12315−12320

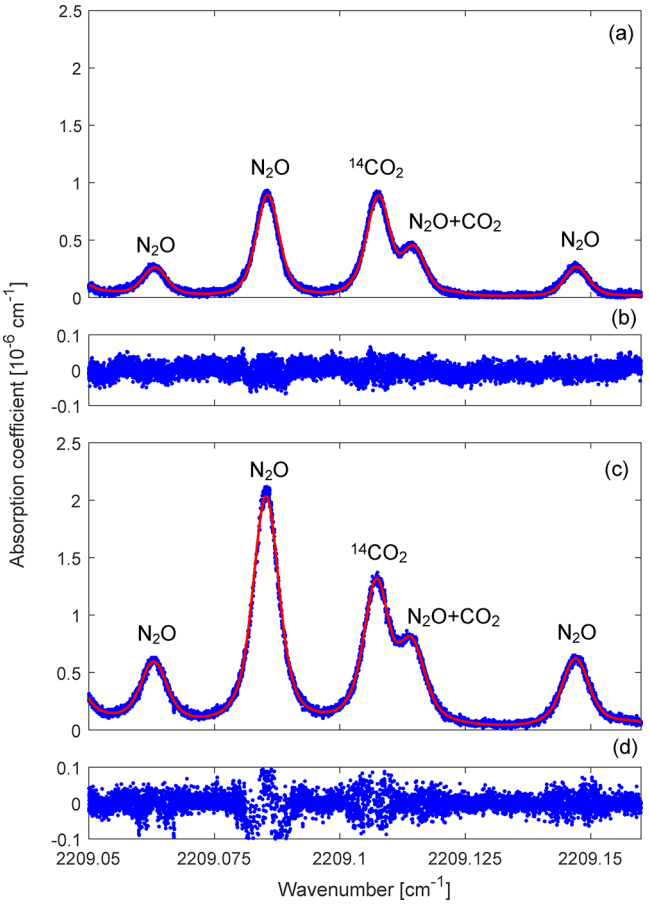

Figure 3. Absorption spectra recorded after CO_2 purification using the sampling system. (a) Only C-14 in the form of CO_2 was detected. (c) Organic radiocarbon was also detected (CO_2+CH_4). In red, fits of the experimental data are shown with their residuals in b and d. Each point corresponds to a ring-down event. Ring-down events exhibiting a too large fit residual were discarded (about 1% of events), as it corresponds to the coupling of higher order modes.

points for each spectrum. In Figure 3a, the pressure reached in the measurement cell was 12.2 mbar, while in Figure 3c it was 17.6 mbar. The pressure was higher due to additional CO_2 produced through the conversion of methane into carbon dioxide. The measurement cell and sample were at room temperature, i.e., 21 °C. Compared to the spectrum shown in Figure 2b, an additional peak is observed, which is the $^{14}CO_2$ absorption line.

The set of 6 measurements was carried out using the procedure described earlier, and the concentrations c_1, c_2, and c_3 were determined for both CO_2 and CO_2+CH_4. The concentrations were calculated by fitting the absorption spectra by a sum of Voigt profiles using a nonlinear least-squares-fitting routine. The obtained fits for the determination of c_1 are shown in red in Figure 3a and 3c, with the corresponding fit residuals in Figure 3b and 3d. In order to correctly model the background other strong absorption lines of CO_2 outside of this wavelength range (situated at 2208.946, 2208.99, 2209.91, and 2209.374 cm^{-1}) were also included in the fitting model.

The obtained concentration values are presented in Table 2. The C-14 activity concentration is calculated in the following way: $\tilde{c} = cp_0/(k_b T t_{1/2} \ln(2))$, with p_0 being the atmospheric pressure and $t_{1/2}$ = 5700 ± 30 years the C-14 half-life.[2,3] These values lead to activity concentrations of 327 Bq/m^3 for $^{14}CO_2$ and 187 Bq/m^3 for $^{14}CH_4$ in agreement with the values from the standard, $\tilde{c}_s$. Similar activity concentration are expected in nuclear facilities, and the achieved sensitivity is thus sufficient for such applications.

Table 2. Results of the Concentration Calculations after Analysis of the Standardized Sample[a]

	$^{14}CO_2$	$^{14}CO_2$+$^{14}CH_4$
p [mbar]	12.2	17.6
c_1 [ppb]	7.4 ± 0.35	8.3 ± 0.4
c_2	0.96 ± 0.03	0.942 ± 0.03
c_3 [ppm]	450 ± 10	610 ± 10
c [ppt]	3.47	5.375
$\tilde{c}$ [Bq/m^3]	327 ± 20	514 ± 30
$\tilde{c}_s$ [Bq/m^3]	339 ± 30	547 ± 35

[a] $\tilde{c}_s$ are the activity concentration values determined conventionally during the preparation of the sample.

The uncertainty of the concentration calculations, listed in Table 2, is derived from the fit residuals, which is the main uncertainty in the measurements. The limit of sensitivity of this system is estimated to be 30 Bq/m^3. In our previous work,[7] a sensitivity of 2 Bq/m^3 is forecast after CO_2 purification. However, this was established without taking into account interferences from neighboring N_2O lines which are currently limiting the sensitivity. Additionally, each measurement step to determine c_1, c_2, and c_3 introduces uncertainties that were not taken into account in our previous work.

CONCLUSIONS

We have demonstrated a full instrumentation for monitoring of elevated C-14 emissions in both organic and inorganic form in atmospheric-like samples. The achieved sensitivity is sufficient for monitoring of fugitive gaseous emissions from nuclear facilities. This work also paves the way for future work on in-situ monitoring of radiocarbon at its natural abundance, which is of great importance for source apportion of CO_2 emissions.

Future efforts will focus on reducing the uncertainty of the measurement, first by improving the removal of N_2O. By using a sensor specifically designed for CO_2 measurement, the absolute amount of carbon dioxide in the sample, c_3, can also be more precisely measured, thus reducing the overall uncertainty of the measurement. Note that for some applications, such as source apportion, only the isotopic ratio needs to be determined, i.e., c_1/c_2, and lower uncertainty could be achieved as c_3 does not need to be measured. Finally, further work will be carried out to reduce the sampling time with a better trap design. Reduction of the size of the instrumentation, in particular, of the sampling system, will lead to future in-situ measurements at a nuclear facility. Increased sensitivity can be achieved by additionally cooling down the samples to reduce the remaining interference of lines from stable isotope CO_2.[18] With these improvements one can envision a similar system to measure C-14 from atmospheric samples below its natural abundance, opening the way to more applications.

AUTHOR INFORMATION

Corresponding Author

*E-mail: guillaume.genoud@vtt.fi.

ORCID

Guillaume Genoud: 0000-0002-5755-5766

Vesa Palonen: 0000-0001-9589-7989

DOI: 10.1021/acs.analchem.9b02496
Anal. Chem. 2019, 91, 12315−12320

Notes

The authors declare no competing financial interest.

■ ACKNOWLEDGMENTS

This work was supported by the Academy of Finland (292756) and is part of the Academy of Finland Flagship Programme, Photonics Research and Innovation (PREIN), decision 320168. It was also funded through the European Metrology Research Programme (EMRP) project "16ENV54−MetroDecom" and the European Metrology Programme for Innovation and Research (EMPIR) project "16ENV09−MetroDecom 2". EMRP and EMPIR are cofinanced by the Participating States and from the European Union's Horizon 2020 research and innovation program.

■ REFERENCES

(1) Management of Waste Containing Tritium and Carbon-14. *Technical Reports Series 421*; International Atomic Energy Agency, IAEA: Vienna, 2004.
(2) Kutschera, W. *Int. J. Mass Spectrom.* **2013**, *349−350*, 203−218. 100 years of Mass Spectrometry.
(3) https://www.nndc.bnl.gov/nudat2/.
(4) Yim, M.-S.; Caron, F. *Prog. Nucl. Energy* **2006**, *48*, 2.
(5) Stenström, K.; Erlandsson, B.; Hellborg, R.; Wiebert, A.; Skog, S.; Vesanen, R.; Alpsten, M.; Bjurman, B. *J. Radioanal. Nucl. Chem.* **1995**, *198*, 203.
(6) Galli, I.; Bartalini, S.; Borri, S.; Cancio, P.; Mazzotti, D.; De Natale, P.; Giusfredi, G. *Phys. Rev. Lett.* **2011**, *107*, 270802.
(7) Genoud, G.; Vainio, M.; Phillips, H.; Dean, J.; Merimaa, M. *Opt. Lett.* **2015**, *40*, 1342.
(8) Galli, I.; Bartalini, S.; Ballerini, R.; Barucci, M.; Cancio, P.; De Pas, M.; Giusfredi, G.; Mazzotti, D.; Akikusa, N.; De Natale, P. *Optica* **2016**, *3*, 385.
(9) McCartt, A. D.; Ognibene, T. J.; Bench, G.; Turteltaub, K. W. *Anal. Chem.* **2016**, *88*, 8714.
(10) Fleisher, A. J.; Long, D. A.; Liu, Q.; Gameson, L.; Hodges, J. T. *J. Phys. Chem. Lett.* **2017**, *8*, 4550.
(11) Sonnenschein, V.; Terabayashi, R.; Tomita, H.; Kato, S.; Hayashi, N.; Takeda, S.; Jin, L.; Yamanaka, M.; Nishizawa, N.; Sato, A.; Yoshida, K.; Iguchi, T. *J. Appl. Phys.* **2018**, *124*, 033101.
(12) Karhu, J.; Tomberg, T.; Vieira, F. S.; Genoud, G.; Hänninen, V.; Vainio, M.; Metsälä, M.; Hieta, T.; Bell, S.; Halonen, L. *Opt. Lett.* **2019**, *44*, 1142.
(13) Bray, C.; Pailloux, A.; Plumeri, S. *Nucl. Instrum. Methods Phys. Res., Sect. A* **2015**, *789*, 43.
(14) Hämäläinen, K.; Jungner, H.; Antson, O.; Räsänen, J.; Tormonen, K.; Roine, J. *Radiocarbon* **2007**, *49*, 325.
(15) Mohn, J.; Szidat, S.; Fellner, J.; Rechberger, H.; Quartier, R.; Buchmann, B.; Emmenegger, L. *Bioresour. Technol.* **2008**, *99*, 6471.
(16) Kratochwil, N. A.; Dueker, S. R.; Muri, D.; Senn, C.; Yoon, H.; Yu, B.-Y.; Lee, G.-H.; Dong, F.; Otteneder, M. B. *PLoS One* **2018**, *13*, e0205435.
(17) Wahlen, M.; Eng, R. S.; Nill, K. W. *Appl. Opt.* **1977**, *16*, 2350.
(18) Labrie, D.; Reid, J. *Appl. Phys.* **1981**, *24*, 381.
(19) Galli, I.; Pastor, P. C.; Di Lonardo, G.; Fusina, L.; Giusfredi, G.; Mazzotti, D.; Tamassia, F.; De Natale, P. *Mol. Phys.* **2011**, *109*, 2267.
(20) Zak, E. J.; Tennyson, J.; Polyansky, O. L.; Lodi, L.; Zobov, N. F.; Tashkun, S. A.; Perevalov, V. I. *J. Quant. Spectrosc. Radiat. Transfer* **2017**, *189*, 267.
(21) Miller, B. R.; Weiss, R. F.; Salameh, P. K.; Tanhua, T.; Greally, B. R.; Mühle, J.; Simmonds, P. G. *Anal. Chem.* **2008**, *80*, 1536.
(22) Mohn, J.; Guggenheim, C.; Tuzson, B.; Vollmer, M. K.; Toyoda, S.; Yoshida, N.; Emmenegger, L. *Atmos. Meas. Tech.* **2010**, *3*, 609.
(23) Palonen, V.; Uusitalo, J.; Seppälä, E.; Oinonen, M. *Rev. Sci. Instrum.* **2017**, *88*, 075102.
(24) Fouladvand, S.; Schernich, S.; Libuda, J.; Grönbeck, H.; Pingel, T.; Olsson, E.; Skoglundh, M.; Carlsson, P.-A. *Top. Catal.* **2013**, *56*, 410.
(25) Yu, F.; Xu, X.; Peng, H.; Yu, H.; Dai, Y.; Liu, W.; Ying, J.; Sun, Q.; Wang, X. *Appl. Catal., A* **2015**, *507*, 109.
(26) Gordon, I.; Rothman, L.; Hill, C.; Kochanov, R.; Tan, Y.; Bernath, P.; Birk, M.; Boudon, V.; Campargue, A.; Chance, K.; Drouin, B.; Flaud, J.-M.; Gamache, R.; Hodges, J.; Jacquemart, D.; Perevalov, V.; Perrin, A.; Shine, K.; Smith, M.-A.; Tennyson, J.; Toon, G.; Tran, H.; Tyuterev, V.; Barbe, A.; Császár, A.; Devi, V.; Furtenbacher, T.; Harrison, J.; Hartmann, J.-M.; Jolly, A.; Johnson, T.; Karman, T.; Kleiner, I.; Kyuberis, A.; Loos, J.; Lyulin, O.; Massie, S.; Mikhailenko, S.; Moazzen-Ahmadi, N.; Müller, H.; Naumenko, O.; Nikitin, A.; Polyansky, O.; Rey, M.; Rotger, M.; Sharpe, S.; Sung, K.; Starikova, E.; Tashkun, S.; Auwera, J. V.; Wagner, G.; Wilzewski, J.; Wcisło, P.; Yu, S.; Zak, E. *J. Quant. Spectrosc. Radiat. Transfer* **2017**, *203*, 3.
(27) Zondervan, A.; Meijer, H. A. J. *Tellus, Ser. B* **1996**, *48*, 601.
(28) Levin, I.; Kromer, B.; Schmidt, M.; Sartorius, H. A novel approach for independent budgeting of fossil fuel CO_2 over Europe by $^{14}CO_2$ observations. *Geophys. Res. Lett.* **2003**, *30*. DOI: 10.1029/2003GL018477
(29) Zak, E. J.; Tennyson, J.; Polyansky, O. L.; Lodi, L.; Zobov, N. F.; Tashkun, S. A.; Perevalov, V. I. *J. Quant. Spectrosc. Radiat. Transfer* **2017**, *203*, 265. HITRAN2016 Special Issue.

DOI: 10.1021/acs.analchem.9b02496
Anal. Chem. 2019, 91, 12315−12320